

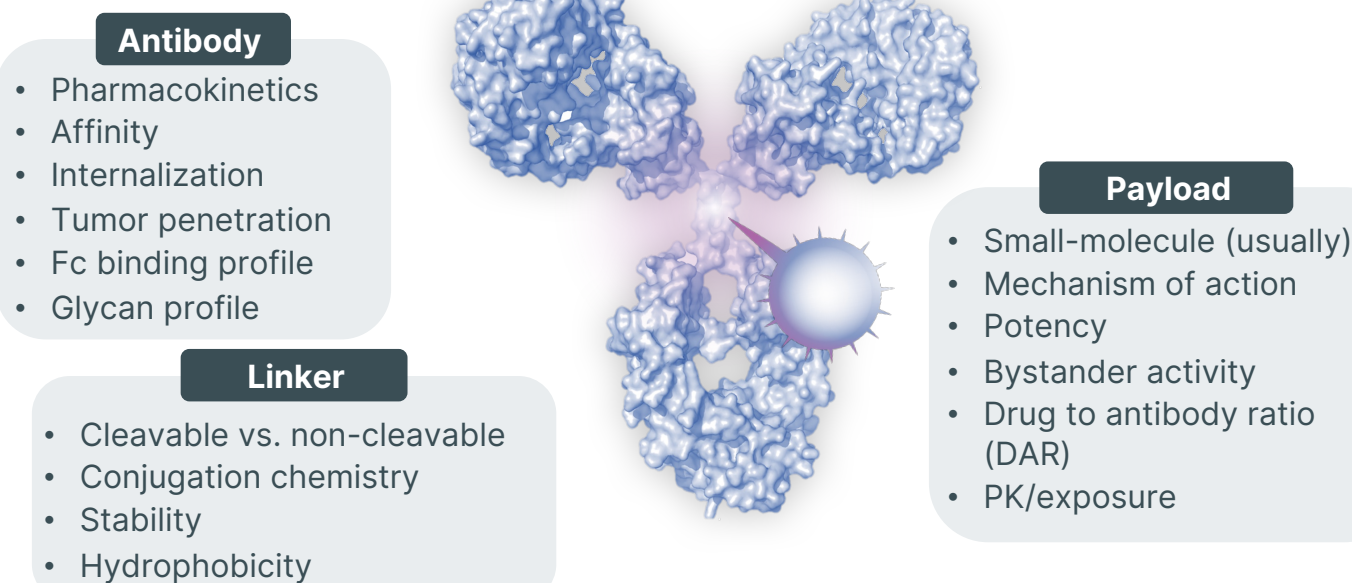
Design and selection of the novel camptothecin analog ZD06519: A payload optimized for antibody-drug conjugates



Michael G. Brant, Mark E. Petersen, Manuel Lasalle, Samir Das, Renee Duan, Jodi Wong, Tong Ding, Kaylee J. Wu, Dayananda Siddappa, Chen Fang, Wen Zang, Alex M. Wu, Truman Hirkala-Schaefer, Graham A. Garnett, Luying Yang, Vincent Fung, Andrea Hernandez Rojas, Samuel Lawn, Catalina Suarez, Stuart D. Barnscher, Jamie R. Rich, Raffaele Colombo
Author affiliations: Zymeworks Inc., Vancouver, BC, Canada

Introduction

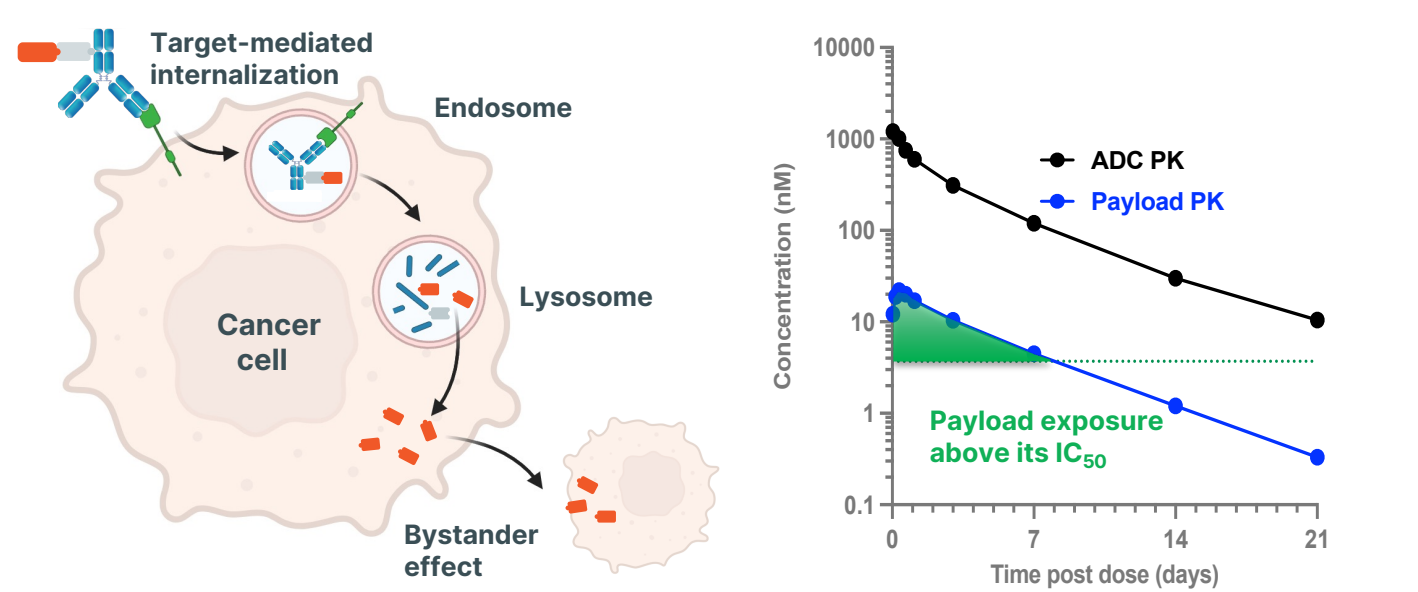
Antibody-drug conjugates (ADCs) have emerged as an effective and promising class of anticancer therapeutics. Over the past 40 years, >370 ADCs have entered the clinic, culminating in 11 FDA approvals to date.



In the clinic, ADCs do not significantly increase the MTD of their conjugated drugs.¹ Instead, when dosed at or near their MTDs, ADCs exhibit higher efficacy compared to their corresponding small molecules.¹

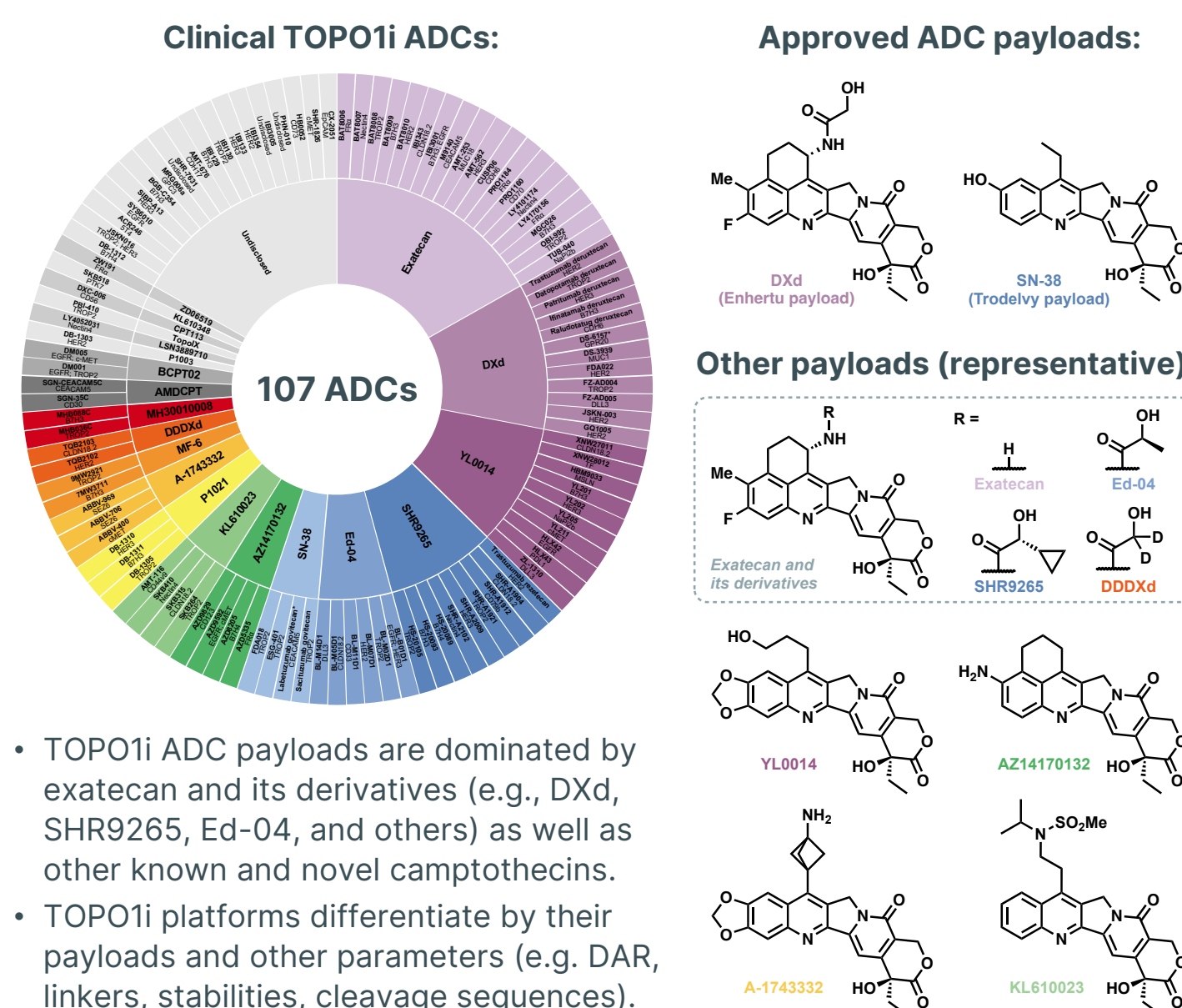
ADC mechanism(s) of action

- Irrespective of the target, radiolabeled antibodies show high normal tissue distribution and generally <1% tumor uptake in humans.²
- ADC efficacy is likely driven by a combination of antigen-mediated (targeted) delivery, bystander effect, and circulating payload exposure.^{1,3}



TOP01i ADC clinical landscape

Historically dominated by microtubule inhibitors, ~half of the ADCs currently in clinical development harbour a topoisomerase-1 inhibitor (TOP01i) payload.



TOP01i ADC payloads are dominated by exatecan and its derivatives (e.g., DXd, SHR9265, Ed-04, and others) as well as other known and novel camptothecins. TOP01i platforms differentiate by their payloads and other parameters (e.g. DAR, linkers, stabilities, cleavage sequences).

Library synthesis, payload in vitro cytotoxicity, and ADC generation

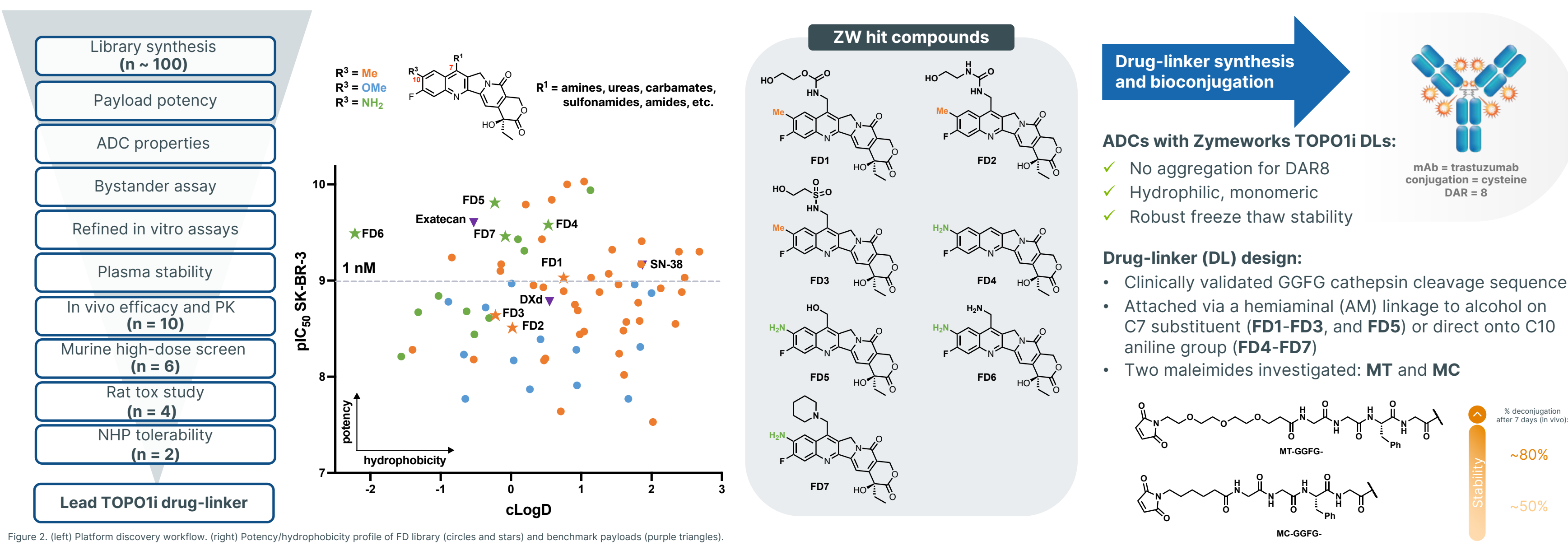


Figure 2. (left) Platform discovery workflow. (right) Potency/hydrophobicity profile of FD library (circles and stars) and benchmark payloads (purple triangles).

Drug-linker structures and in vitro potency of HER2 conjugates (bystander assay)

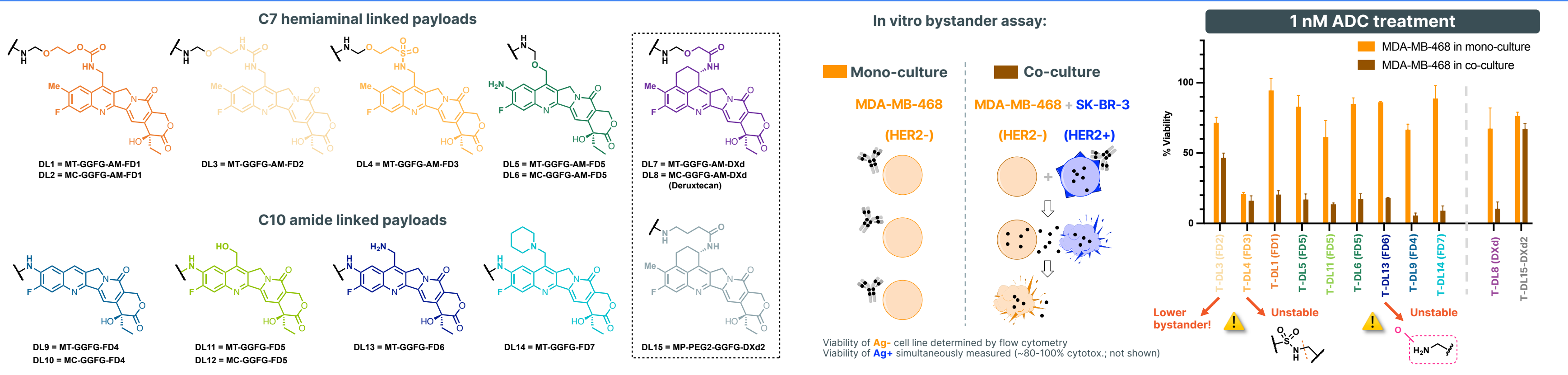


Figure 3. Structures of C7 hemiaminal (AM) linked payloads, C10 amide-linked payloads and controls (DXd and DXd2 drug-linkers).

Figure 4. Viability of antigen negative MDA-MB-468 cells treated with 1 nM ADC when grown in monoculture (orange) or in co-culture with high HER2 expressing SK-BR-3 cells (brown). T-DL3 (FD3) and T-DL13 (FD6) showed instability in mouse plasma after 7 days, other DLs showed no instability after 7 days.

In vitro spheroid assay, in vivo efficacy in JIMT-1 (HER2 ADCs), and rodent tolerability (FRa ADCs)

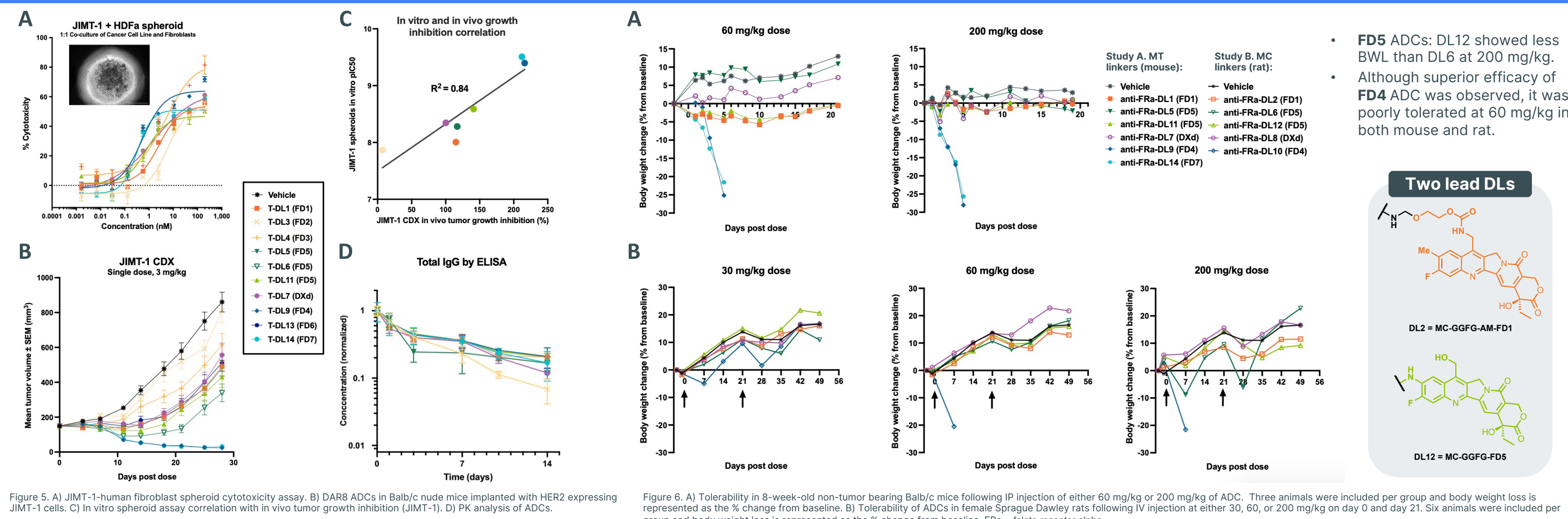


Figure 5. A) JIMT-1-human fibroblast spheroid cytotoxicity assay. B) DAR8 ADCs in Balb/c nude mice implanted with HER2 expressing JIMT-1 cells. C) In vitro spheroid assay correlation with in vivo tumor growth inhibition (JIMT-1). D) PK analysis of ADCs.

Figure 6. A) Tolerability in 8-week-old non-tumor bearing Balb/c mice following IP injection of either 60 mg/kg or 200 mg/kg of ADC. Three animals were included per group and body weight loss is represented as the % change from baseline. B) Tolerability of ADCs in female Sprague Dawley rats following IV injection at either 30, 60, or 200 mg/kg on day 0 and day 21. Six animals were included per group and body weight loss is represented as the % change from baseline. FRa = folate receptor alpha.

NHP tolerability and lead selection

DL2 (FD1) chosen as lead drug-linker platform for its superior tolerability at 120 mg/kg (DAR4) versus DL12 (FD5).

Group	Test Article	DAR	Dose (mg/kg)	Tolerated?
1	Vehicle	-	-	Y
2	mAb-DL7 (DXd)	8	30	Y
3		80	N	
4		60	Y	
5	mAb-DL2 (FD1)	4	120	Y
6		8	30	Y
7		80	N	
9	mAb-DL12 (FD5)	4	60	Y
10		8	120	N
11		8	30	Y
12	8	80	N	

Weeks: 0, 1, 2, 3, 4. Drug Dose at weeks 1, 3, 4. Necropsy at week 4.

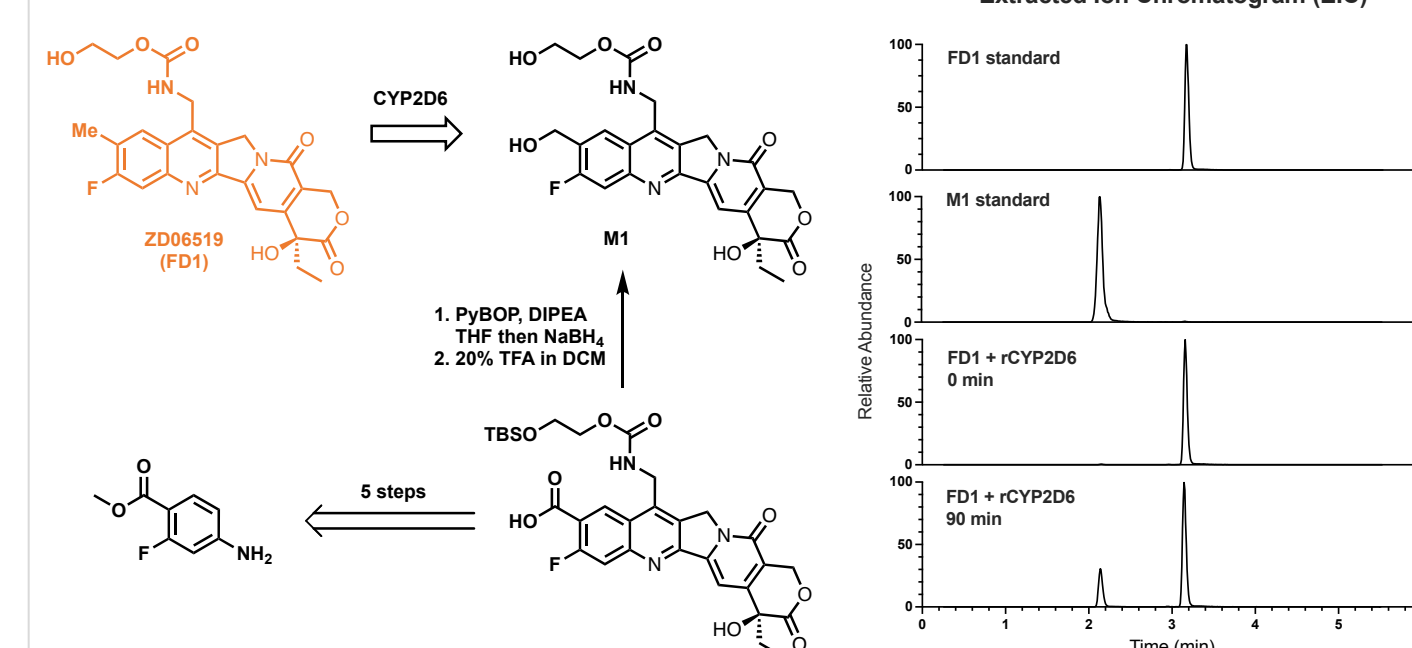
Table 1. DL2 (FD1) and DL12 (FD5) evaluated in a two-dose non-GLP NHP toxicology study (at both DAR4 and DAR8) and compared with DAR8 DL7 (DXd).

Metabolism of FD1 (ZD06519)

- M7 is major metabolite in rodents and monkeys; M1 in human microsomes.
- CYP profiling revealed FD1 is a substrate for CYP2D6.

Peak No.	R.T. (min)	m/z [M+H] ⁺	Mass shift (Da)	Mass error (ppm)	Biotransformation	Percentage peak area at 90 min (MS)			
						Mouse	Rat	Monkey	Human
M1	6.60	514.162	15.994	0.3	Mono-hydroxylation	0.40%	0.1%	2.8%	18.9%
FD1	8.14	498.166	0.000	-0.3	Parent drug	90.0%	92.6%	78.4%	72.8%
M7	10.64	452.161	-46.005	-1.2	Hydrolysis + de-carboxylation + de-hydration + de-hydrogenation	5.8%	2.2%	8.3%	3.5%

Table 2. Major (>2%) metabolites of FD1 in microsomes.



Summary and conclusions

- FD1 (ZD06519) was selected from a library of ~ 100 compounds, based on its favorable in vitro ADME/DMPK profile, in vivo efficacy and superior tolerability observed in rodents and NHP.
- Investigational new drug (IND) application for ZW191 (FRa ZD06519 DAR8 ADC) cleared by FDA in July 2024.
- GPC3 (ZW251) and NaPi2b (ZW220) ADC INDs planned for 2025.

Poster adapted from: M. E. Petersen, M. G. Brant et al. *Mol. Cancer Ther.* 2024, 23, 606-618.

References:
1. R. Colombo and J. Rich. *Cancer Cell*, 2022, 40, 1255-1263.
2. F. Bensch et al. *Theranostics*, 2018, 8, 4295-4304.
3. E. Tarcsa et al. *Drug Discov. Today. Technol.* 2020, 37, 13-22.